

The Method of Curvature Attribute applied in the Depth Inversion of the Geological Bodies Edge by Potential Field Data

Jinlan Liu¹, Wanyin Wang^{1*}, Shengqing Xiong²

*1 Institute of Gravity and Magnetic Technology, Chang'an University, Xi'an, China
(liujl_dc@163.com, wwy7902@chd.edu.cn)*

*2 China Aero Geophysical Survey & Remote Sensing Center for Natural Resources, Beijing,
China (xsq@agrs.cn)*

2020 05 05

1 Introduction

2 Methodology

3 Three Key Techniques

**4 Tests on Synthetic Data and
Application to Actual Data**

5 Conclusion

The application of curvature to source edge recognition and depth inversion of potential field was developed in the past 20 years.

Many geophysicists have made many contributions in this field, such as:

R.O. Hansen et al., 2006; Jeffrey D. Phillips et al., 2007; Jinlan Liu, 2008; Xu Zhang et al., 2012; Cevallos et al. 2012 and 2013; Wenna Zhou et al. 2013; Barraud, J., 2013; Jingtian Tang et al., 2019.

However, there are still some problems in this method, such as:

- The continuity of the inversion solution needs to be further strengthened;**
- The accuracy of depth inversion needs to be further improved;**
- In order to solve the problem that the curvature property is sensitive to the high frequency interference, it is urgent to find a stable screening technique for the inversion solution.**

Roberts (2001) gives the curvature function as: Roberts (2001) gives the curvature formula of any function $F(x)$:

$$K(x) = \frac{d^2 F / dx^2}{\left(1 + (dF / dx)^2\right)^{3/2}}$$

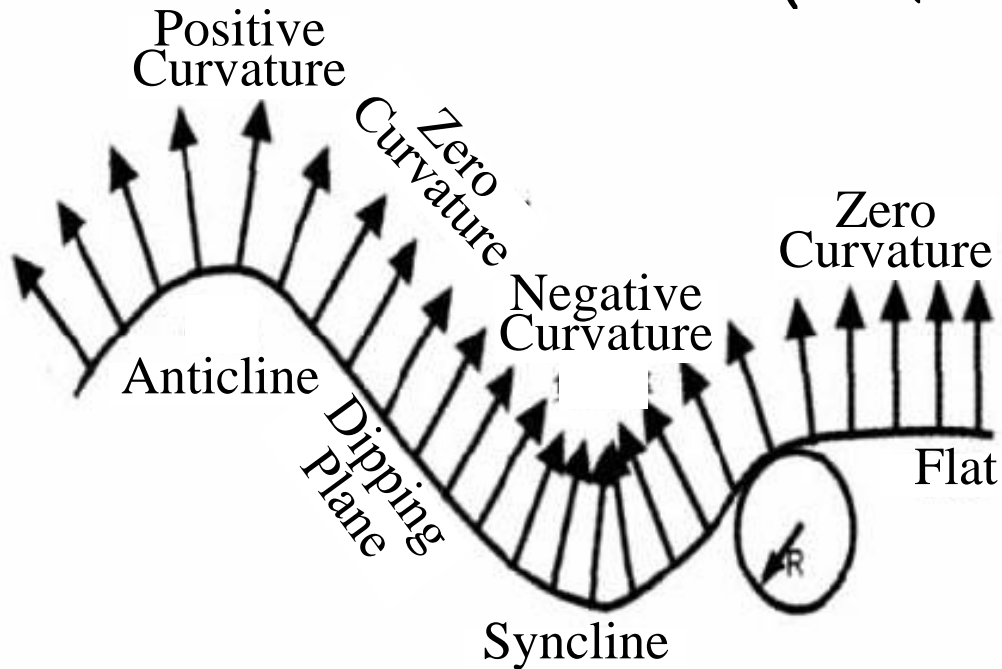
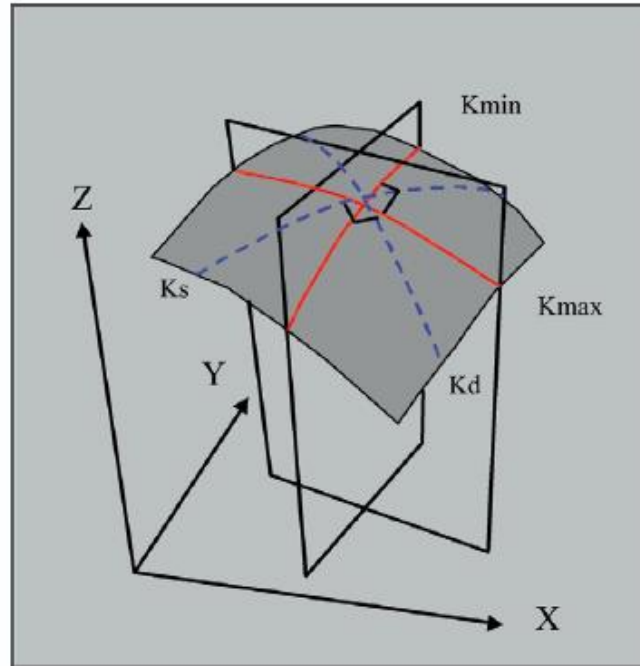


Fig.1 Sign convention for curvature attributes
(Roberts, 2001)



Kmax:
maximum curvature

Kmin:
minimum curvature

Kd:
dip curvature

Ks:
strike curvature

K_+ :
most positive curvatures

K_- :
most negative curvatures–

Fig.2 Curvature in three-dimensions
(Mario, 2003)

The basic principles of potential field source edge position and depth inversion based on the curvature attribute are as follows:

- Special function $S(x, y)$ can be obtained by processing and transforming the data of the gravity and magnetic anomalies (such as the total horizontal derivative THDR of gravity anomaly and RTP magnetic anomalies, analytic signal amplitude ASM, etc.).
- The special function $S(x, y)$ has the peak value or the ridge value $S(x_0, y_0)$ at the point (x_0, y_0, z) above the edge of the field source body (such as contact zone, fault, rock mass, etc.).
- Using this peak or ridge value $S(x_0, y_0, z)$ and the minimum negative curvature $K_-(x_0, y_0, z)$ at the peak, the buried depth of the top surface on the edge of the source body of the potential field can be estimated.

The relation between the buried depth Z and the minimum negative curvature K_- at the edge of the field source is as follows (D. Phillips et al, 2007):

$$Z = \sqrt{-\frac{2\beta S(x_0, y_0, z)}{K_-(x_0, y_0, z)}}$$

K_- is called the "most negative curvature" by Roberts (2001); β is a constant, and according to D. Phillips et al. (2007), the value is 1 in the paper. (x_0, y_0) is the point coordinate above the edge of the field source body.

3.1 The optimal solution problem of objective function

The optimal solution of the objective function is the key algorithm of curvature attribute extraction. The Huber norm is introduced into the extraction algorithm of curvature attribute, which make the edge depth of the geological body more accurate than the L_2 norm (the traditional least square method).

$$g(x, y) \approx a + bx + cy + dx^2 + exy + fy^2$$

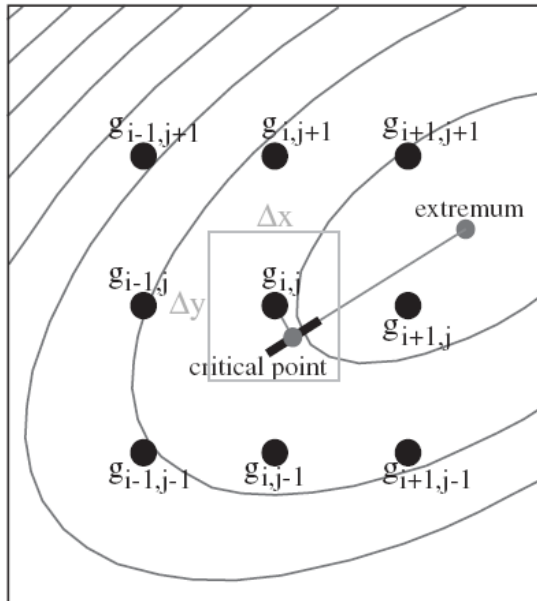


Fig.3 Quadric fitting map for determining ridged tops of specific functions (according to Phillips, 2007)

Suppose the linear system $d = Am$, where d is the observation data A is the forward operator, m is the model parameter vector, as follows:

$$m = (a, b, c, d, e, f)^T$$

Target equation based on the L_2 norm (Least square method):

$$f(m) = \|Am - d\|_2 = \|r\|_2 = \sum_{i=1}^M \sum_{j=1}^N M_\varepsilon(r_{ij})$$

Target equation based on Huber norm (L_1 and L_2 mixture norm):

$$f(m) = \|Am - d\|_{Huber} = \|r\|_{Huber} = \sum_{i=1}^M \sum_{j=1}^N M_\varepsilon(r_{ij})$$

3 Three Key Techniques

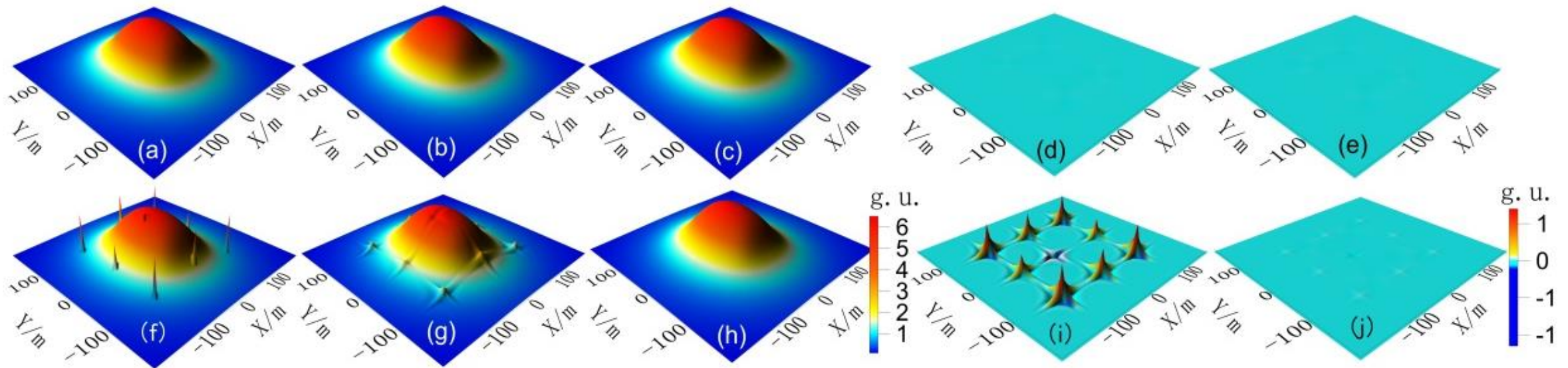


Fig.4 The surface fitting effect contrast of the theoretic surface for potential field and the noisy surface by Huber norm method and the L_2 norm

(a) Theoretical gravity anomaly derived from a single prism; (b) The surface fitting result of fig.4a by the L_2 norm; (c) The surface fitting result of fig.4a by Huber norm; (d) The residual of b-a; (e) The residual of c-a; (f) Add 9 interference points to the theoretical gravity anomaly of fig.4a ; (g) The surface fitting result of fig.4f by the L_2 norm; (h) The surface fitting result of fig.4f by Huber norm; (I) The residual of g-a; (j) The residual of h-a.

3 Three Key Techniques

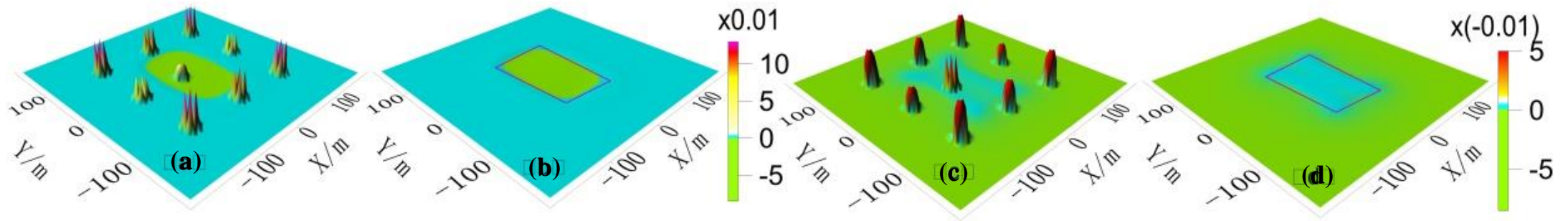


Fig.5 The extraction of curvature attributes from fitting surface with interference model of fig.4f (purple box is the theoretical edge position of geological body)

- (a) The extraction of maximum curvature by L_2 norm; (b) The extraction of maximum curvature by the Huber norm; (c) The extraction of minimum negative curvature by L_2 norm; (d) The extraction of minimum negative curvature by Huber norm.

The above experiments further illustrate that the Huber norm has **better anti-interference effect**, the fitted surface is **more accurate** and the extracted curvature properties are **more in line with the reality**.

3.2 Solution continuity problem

The continuity problem of the depth solution of the field source edge is studied, and the normalized total horizontal derivative vertical derivative technology (NVDR-THDR) (Wanyin Wang et al, 2009) is introduced into this method, so that the edge position of the geological body corresponding to the depth solution of the inversion by the NVDR-THDR technology is more continuous than the result by the THDR technology, and the recognition rate of the small-scale structure edge is higher.

3 Three Key Techniques

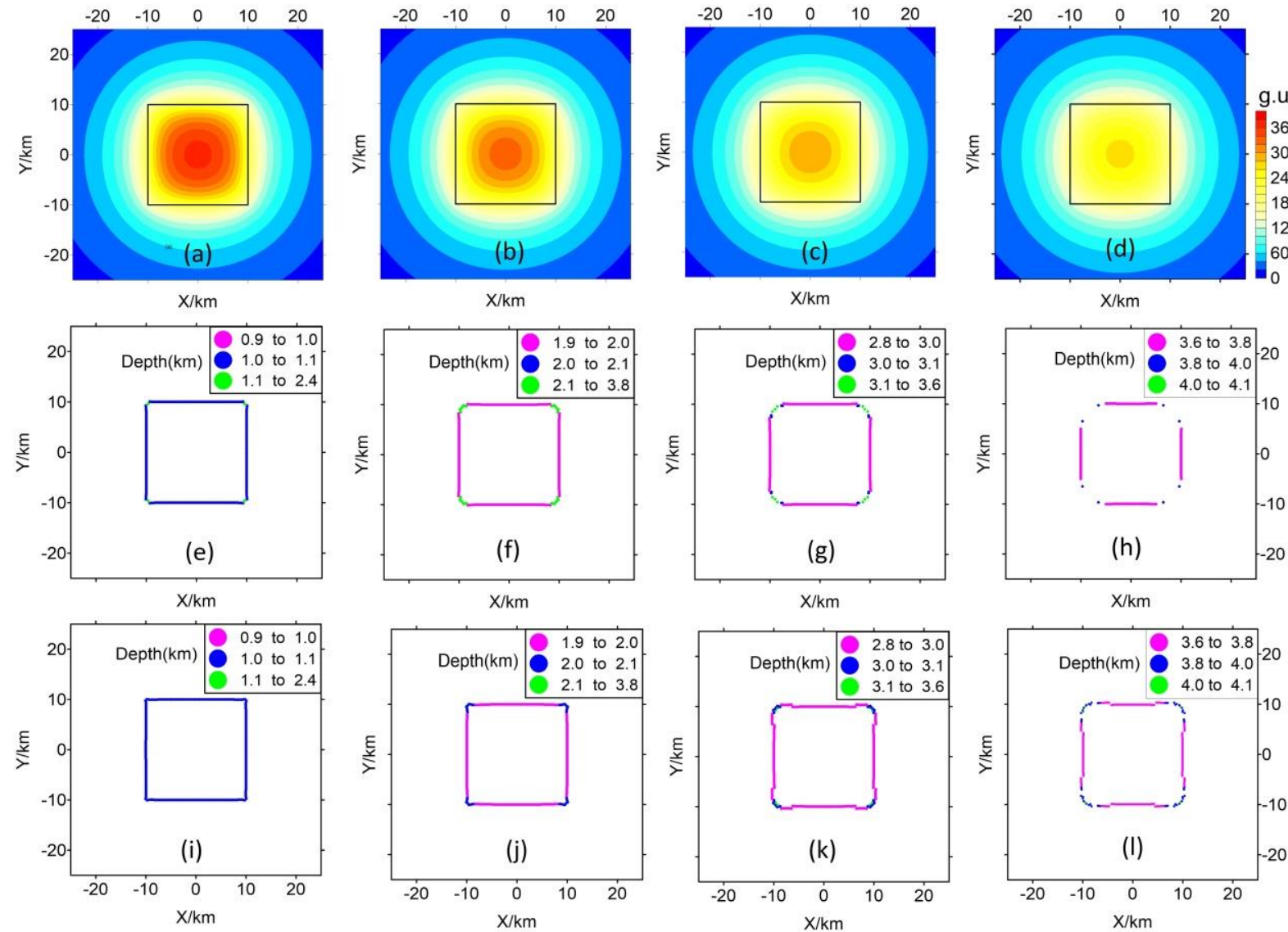


Fig.6 The edges depth inversion results of the vertical prisms with different buried depths based on the curvature attribute using THDR and NVDR- THDR of the gravity anomaly (a)~(d) Theoretical gravity anomaly of prismatic body with buried depth range of 1-20km, 2-21km, 3-22km and 4-23km respectively (the black box is the edge position of the prism). (e)~(h) The edges depth inversion results of the theoretical gravity anomaly of fig.6(a)~(d) based on the curvature attribute (THDR source data); (I)~(l) The edges depth inversion results of the theoretical gravity anomaly of fig.6(a)~(d) based on the curvature attribute (NVDR-THDR source data).

3 Three Key Techniques

$$\varepsilon = \sqrt{\frac{1}{M} \sum_{i=1}^M \left(\frac{A_i - B_i}{h_i} \right)^2}$$

A_i is the inversion depth based on curvature attribute inversion;
 B_i is the theoretical depth;
 h_i is the theoretical depth;
 M is the total number of depth points involved in the calculation.

Table 1 The relative mean square error statistical table for the ratio of the deviation (between inversion depth and theoretical depth) and the theoretical depth using THDR and NVDR- THDR of the gravity anomaly

The buried deep of the prism top(km)	1	2	3	4	
error	THDR	4.00%	4.22%	4.95%	7.04%
	NVDR-THDR	2.42%	2.40%	3.91%	5.60%

The above experiments further illustrate that The NVDR-THDR source data is introduced to replace the traditional THDR data, which greatly improves the continuity and accuracy of edge position recognition of geological bodies (especially geological bodies with deep buried depth) and the precision of edge burial depth inversion.

3.3 The screening problem of solution

Curvature is a method based on the second derivatives. As a result, the curvature property is very sensitive to small structures, but at the same time, it is sensitive to any noise pollution coming from underground.

The upward continuation technique at a certain height is introduced to suppress interference in the inversion process, and **the actual inversion depth can be obtained by subtracting the upward continuation height from the final inversion depth(Li Cui, Wanyin Wang, 2011)**

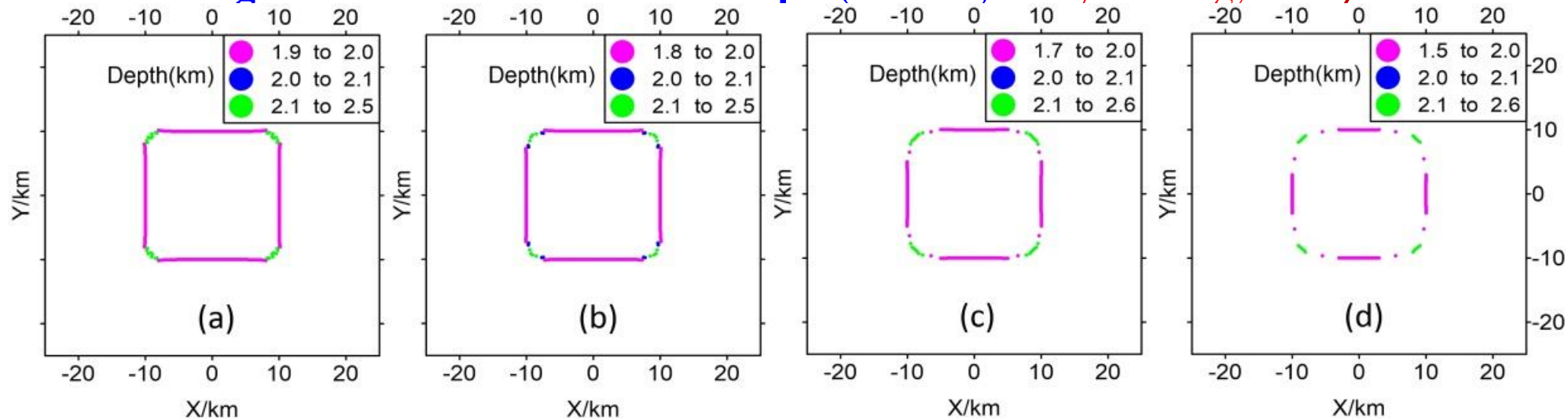


Fig. 7 Influence of different heights of upward continuation on the inversion depth of curvature attributes
(the upper top surface depth of the theoretical model is 2km)
(a) 0.5km; (b) 1.0km; (c) 2.0km; (d) 3.0km.

4.1 Tests on Synthetic Data

Table 2 The position coordinates and physical parameters of the five models

Model number	The upright prism coordinates of the angular point(10^3m)						magnetization J ($10^{-3}\text{A}\cdot\text{m}^{-1}$)	Magnetization Angle I ($^{\circ}\text{N}$)	Magnetic declination D ($^{\circ}\text{E}$)	Residual density σ (kg/m^3)
	x1	x2	y1	y2	z1	z2				
A1	6	8	16	17	0.4	0.8	11000	90	0	250
A2	5	7	5	6.5	1.5	2	9000	90	0	500
A3	13	14	11	13	0.5	0.9	11000	90	0	300
B1	10	20	9	16	1.5	3	23000	90	0	-100
B2	5	9	12	20	1.5	3	22000	90	0	250

B1 and **B2** models are buried deeper and larger in scale;
A1, **A2** and **A3** models are small in size and shallow in depth;
A2 is the weak anomaly model (**small scale and large buried depth**)

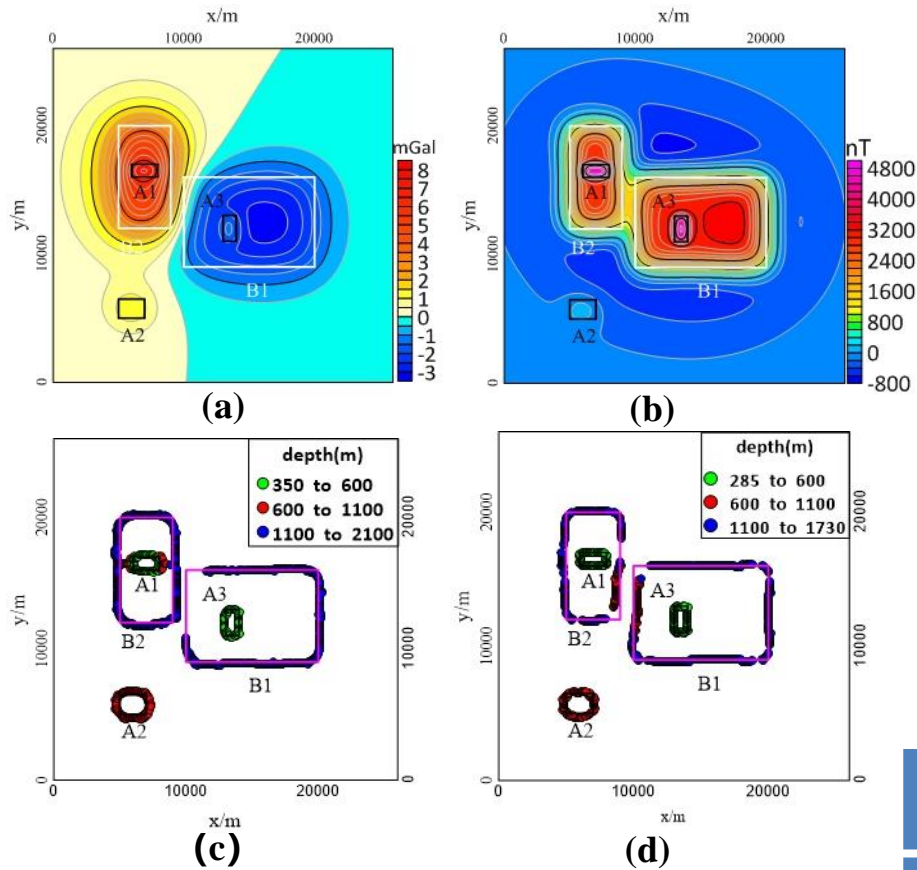


Fig. 8 Theoretical gravity and magnetic anomalies of the five models on the observation plane $Z=0.0\text{m}$ and the inversion depth results based on the curvature attribute

(the squares show the theoretical plane positions of five models)

- (a) Gravity anomaly map; (b) RTP magnetic anomaly map;
- (c) Inversion results of gravity anomaly; (d) Inversion results of RTP magnetic anomalies.

Table 3 The relative mean square error statistical table for the ratio of the deviation (between inversion depth and theoretical depth) and the theoretical depth for the gravity anomaly of five models

Model		A1	A2	A3	B1	B2	综合误差
Error	Gravity anomaly	7.40%	12.44%	5.35%	9.38%	8.82%	8.68%
	RTP magnetic anomaly	5.63%	13.22%	7.95%	17.6%	13.74%	11.63%

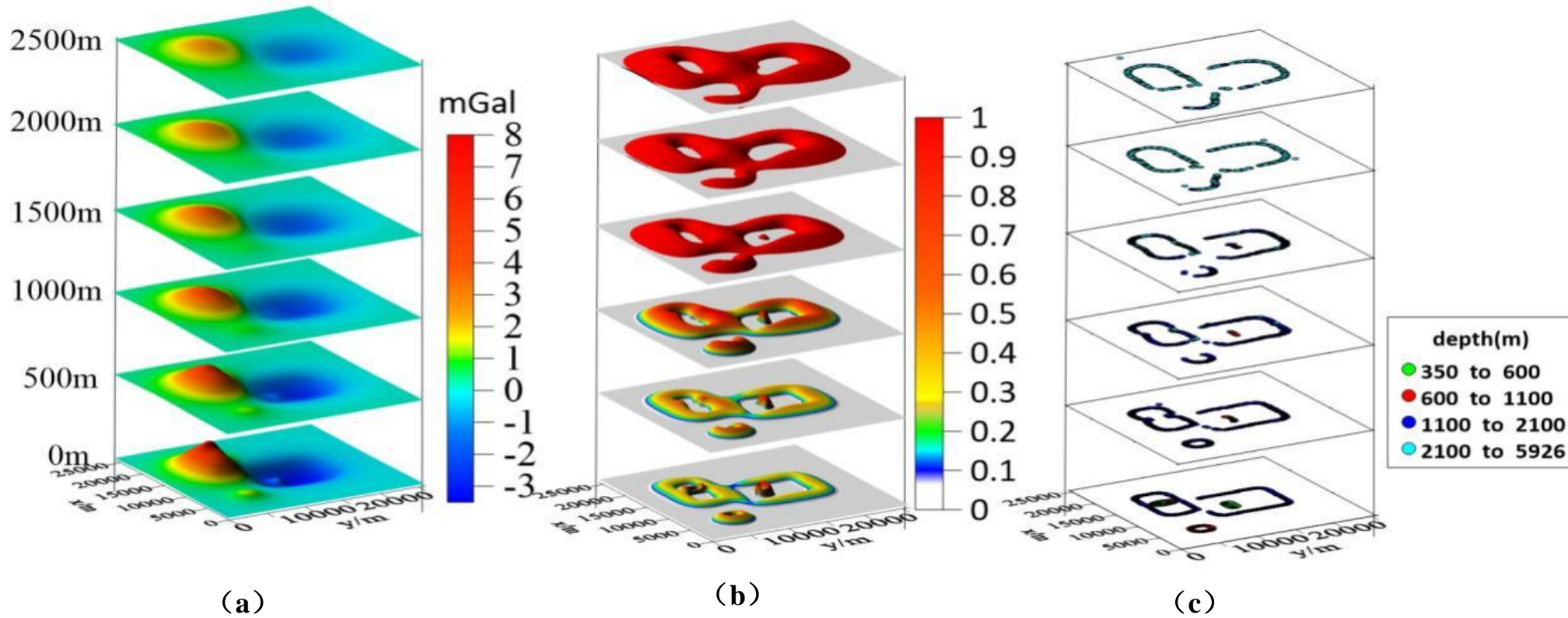


Fig.9 Gravity anomalies, NVDR-THDR recognition results and depth inversion results based on curvature attribute of the five models at different heights

- (a) Gravity anomalies map;
- (b) NVDR-THDR recognition results of gravity anomalies;
- (c) Inversion depth results of gravity anomalies based on curvature properties.

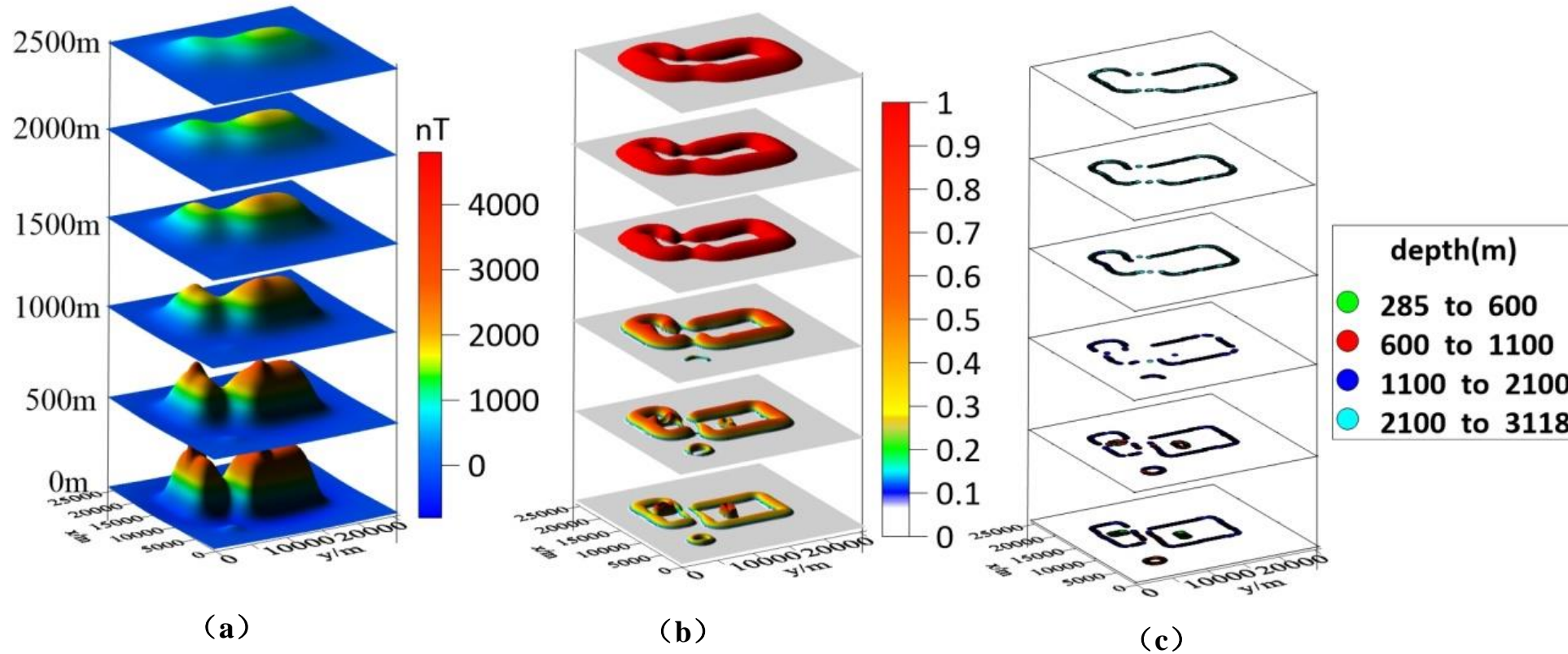
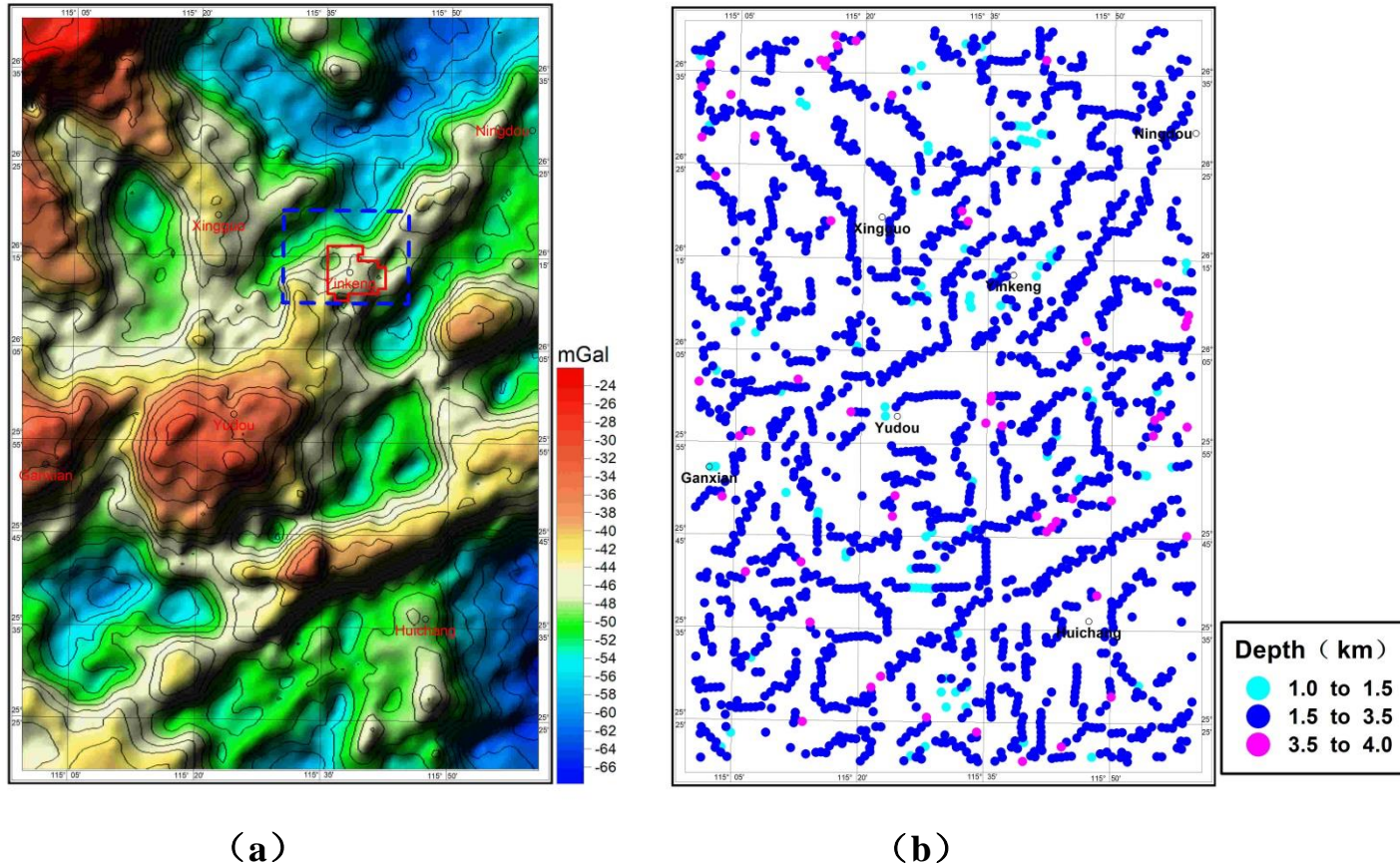


Fig.10 RTP magnetic anomalies, NVDR-THDR recognition results and depth inversion results based on curvature attribute of the five models at different heights
 (a) RTP magnetic anomalies map; (b) NVDR-THDR recognition results of RTP magnetic anomalies; (c) Inversion depth results of RTP magnetic anomalies based on curvature properties.

4.2 Application to Actual Data



The inversion solution is relatively continuous, and the fault depth of the top surface is basically the same, with most of the depth between 1.5 and 3.5km.

**Fig.11 (a) Gravity anomalies map in Yudu-Ganxian area of Nanling in China;
 (b) Inversion depth of the fault top surface based on curvature properties.**

- In this paper, **three key techniques** of edge depth inversion of potential field source based on curvature attribute are studied: **the optimal solution problem of objective function, the edge position problem of geological body and the screening problem of solution.**
- Through the above three key techniques, **the accuracy, continuity and recognition rate to the small-scale structure of the inversion result are optimized.**
- The theoretical model is used to verify the effects of the above key technologies, the results show that the three key technologies have achieved good results, and the combined model is used to verify the effect of the optimized inversion method.
- The measured aeromagnetic data were used to inverting the edge depth of the intrusive rock in a mining area, and **the inversion results are in good agreement with the rock depth revealed by borehole.**